The editorial version of the paper can be found at IEEE Trans. on Ind. Electron., ISSN 0278-0046, Vol. 65, No. 1, pp. 907 – 917

Eprint: https://doi.org/10.1109/TIE.2017.2726970

To cite this paper: Pilloni, A., Pisano, A. and Usai, E., 2017. Robust finite-time frequency and voltage restoration of inverter-based microgrids via sliding-mode cooperative control. *IEEE Transactions on Industrial Electronics*, *65*(1), pp.907-917.

Robust Finite Time Frequency and Voltage Restoration of Inverter-based Microgrids via Sliding Mode Cooperative Control

Alessandro Pilloni, Alessandro Pisano, *Member, IEEE*, and Elio Usai, *Member, IEEE*

***Abstract*—In this paper, we present a novel control strategy to perform the exact finite-time restoration among voltages and frequencies of an islanded inverter-based microgrid. The problem is attacked from a cooperative-based control perspective inspired to the tracking consensus paradigm. Ad-hoc chattering-free sliding-mode based distributed algorithms are designed to enhance the underlying robustness and convergence properties of the system with respect to the existing solutions. Particularly, the restoration is achieved while dispensing with the knowledge of the distributed generators' models and parameters. Performance of the control system is analyzed by Lyapunov tools, and a simple set of tuning rules are derived. The effectiveness of the proposed scheme is verified by simulations on a realistic inverter-based microgrid modelization.**

***Index Terms*—Distributed control, consensus algorithms, inverters, microgrids, secondary control, sliding mode control.**

Robust Finite Time Frequency and Voltage Restoration of Inverter-based Microgrids via Sliding Mode Cooperative Control

Alessandro Pilloni, Alessandro Pisano, *Member*, *IEEE*, and Elio Usai, *Member*, *IEEE*

***Abstract*—In this paper, we present a novel control strategy to perform the exact finite-time restoration among voltages and frequencies of an islanded inverter-based microgrid. The problem is attacked from a cooperative-based control perspective inspired to the tracking consensus paradigm. Ad-hoc chattering-free sliding-mode based distributed algorithms are designed to enhance the underlying robustness and convergence properties of the system with respect to the existing solutions. Particularly, the restoration is achieved while dispensing with the knowledge of the distributed generators' models and parameters. Performance of the control system is analyzed by Lyapunov tools, and a simple set of tuning rules are derived. The effectiveness of the proposed scheme is verified by simulations on a realistic inverter-based microgrid modelization.**

***Index Terms*—Distributed control, consensus algorithms, inverters, microgrids, secondary control, sliding mode control.**

I. Introduction

MICROGRIDs (MGs) constitute the bridge between the traditional electrical distribution system and the distributed renewable generation [1]–[3]. While often connected to larger grids, MGs can autonomously "insland" themselves in response to pre-planned or unplanned events and then operate independently. During grid-tied operation the MG control is simple, since the larger primary grid dominates the MG dynamics. On the contrary, in islanded operation the MG control is crucial for a reliable power delivery and to preserve synchronization, voltage stability and load sharing [3].

To simplify the system's integration, the MG control infrastructure is recently standardized into a three-layer hierarchical architecture [4]–[6]. The *Primary Control* (PC), depicted in Fig. 1, consists of local controllers acting on each Distributed Generator (DG) to preserve the MG stability while guaranteeing the load sharing facilities. The *Secondary Control* (SC) designed to compensate the unavoidable deviations of the DG's output voltages and frequencies from the expected setpoints. The *Tertiary Control* (TC), with the aim to guarantee a correct and economical power dispatching.

Manuscript received November 3, 2016; revised January 29 and April 19, 2017; accepted June 15, 2017. This work was supported by the Sardinia Region Governement L.R.7/2007, CRP-7733 and by the Fondazione di Sardegna, CUP:F72F16003170002. A. Pilloni, A. Pisano and E. Usai are with the Dipartimento di Ingegneria Elettrica ed Elettronica (DIEE), Università degli Studi di Cagliari, Cagliari, 09123, Italy. E-mail addresses: alessandro.pilloni@diee.unica.it; pisano@diee.unica.it; eusai@diee.unica.it.

A. Literature review

This research is focused on designing a novel SC layer. Centralized approaches to SC design have been firstly proposed in [2]. However, the current trend is to discourage centralized strategies [6] whose disadvantages are, e.g.: 1) latency and delays due to all-to-one communication; 2) the need of costly central computing and communication units; 3) poor global reliability of the power system due to critical sensitivity to single-point failures. Additionally, they are hardly scalable, not flexible, and do not possess plug-and-play functionalities.

To overcome these limitations, multi-agent based consensus controllers have been proposed to take advantage of their inherent scalability and flexibility features [7] to address power dispatch [8], [9] and secondary voltage and frequency restoration problems [10]–[16] in the distributed control setting. In [10] the secondary distributed voltage and frequency restoration task is addressed. However, due to the requirement of all-to-all communication among DGs, its communication overhead was significantly greater than that of the centralized strategies [2]. Furthermore, no formal stability analysis was made. Among the existing investigations, references [11]–[16] appear to be the more closely related to the present research.

An overview of the main features of these proposals as well as the main improvements provided by the present paper are explained hereinafter.

Frequency restoration: Based on Distributed Averaging Proportional Integral (DA-PI) scheme, [11] proposes for the first time the use of the consensus paradigm to restore the frequencies in an islanded MG. The results are derived on the basis of a simplified MG model consisting of coupled Kuramoto oscillators. A different strategy, namely a consensus-based Distributed Tracking (DT) approach, is proposed in [12]. Both papers [11], [12] implement active power sharing functionalities, but the corresponding approaches only possess local exponential stability properties. Additionally, in [11] the restoration frequency ω_{ref} must be constant and globally known to all DGs. On the contrary, [12] allows to arbitrarily modify the steady frequency of the MG by simply acting, at the local level, on a particular DG referred as "leader".

Note that, although the leader information is available only to a small portion of DGs, the whole MG will cooperatively converge towards the expected synchronization value in spite of limited communications [17]. This feature is particularly useful during islanded operation when more active power is required, or to seamlessly transfer the MG from islanded to grid-connected mode [18].

Voltage restoration: Similarly, DA-PI and DT solutions have also been employed for voltage restoration purposes. The DA-PI approach in [13] is only capable of providing a tuneable compromise between the adverse tasks of voltage restoration and reactive power sharing accuracy. Furthermore, as in [11], such an approach doesn't allow to arbitrarily affect the restoration voltages. Other solutions can be found in [3], [19], [20]. However, none of them provide guidance in characterizing the power sharing properties with respect to the voltage restoration accuracy. On the contrary, since national agencies penalize customers with low load power factors, DT schemes [12], [14]–[16] focus on the exact voltage restoration problem only, disregarding the reactive power sharing issue.

Common approach is to convert the voltage restoration problem into a linear DT consensus problem by using feedback linearization techniques. Then, after linearization, the exact voltage restoration can be achieved by using different DT consensus strategies, such as, for instance, power fractional finite-time control [12], linear proportional-derivative [14], ARE-based [15], and sliding-mode (SM) based adaptive neural networks [16]. Among them, it is worth to mention that only [16] considers the presence of uncertainties and unmodeled dynamics in its treatment.

Clearly, the underlying requirement of feedback linearization techniques to have an exact MG mathematical model is rather unrealistic in practical scenarios, and furthermore feedback linearization may also yield numerical problems (e.g. due to the online computation of nonlinear coordinate transformations or high-order Lie Derivatives) that can compromise the effectiveness of the whole control system.

B. Statement of contributions

Inspired by the most recent results in the area of SM-based DT consensus [21], [22], we propose a novel SC layer capable of providing the finite-time voltage and frequency restoration in an islanded inverter-based MG. In contrast with the existing DT solutions, our implementation does not rely on the knowledge of the DGs' mathematical models (i.e., the present proposal is inherently robust against model/parameter uncertainties) and it dispenses with the need to measure several grid variables and parameters, cfr. [12], [14]–[16].

Particularly, the proposed DT frequency restoration SC improves the performances of the DA-PI controller in [11] since it allows to arbitrarily modify in a distributed way the MG frequency by acting on the leader DG only. Furthermore, the scheme in [12] is also overperformed in terms of convergence rate (that was exponential in the quoted references [11], [12] whereas the present work provides finite-time convergence properties). A dedicated Lyapunov analysis based on a faithful nonlinear modelization of MG corroborates the finite-time stability "in-the-large" of the proposed scheme without relying on local linearization arguments. The analysis confirms that the active power sharing constraints are restored in finite-time even in spite of abrupt modifications of the power demand.

The present investigation additionally proposes a novel SM based DT scheme for the voltage restoration. In contrast with the existing solutions the present proposal dispenses with the use of feedback linearization techniques, that were employed, respectively, in [12], [14]–[16].

In both the proposed frequency and voltage SM-based SCs, chattering is alleviated by relying on ad-hoc input dynamic extension technique where the discontinuous sign functions only appear in the time derivatives of the actual control input, thus yielding continuous control actions. The proposed SCs thus inherit all the main desirable properties of SM control, such as finite-time convergence, high accuracy, and robustness to uncertainties, disturbances and unmodeled dynamics, without being affected by the chattering phenomenon.

Particularly, to figure out what can be expected when the proposed methods will be applied to an actual MG, we notice that robustness to realistic measurement noise and parameter uncertainty/variations has been verified by simulations. Unmodeled dynamics of the grid components will be the main issue arising at the practical implementation stage, causing an increase in the input-output relative degrees. It is well known, however, that sliding-mode controllers possess significant robustness properties against the presence of sufficiently fast unmodeled dynamics, that should be the case in the applicative scenario of MG control under investigation.

C. Paper organization

Section II presents the nonlinear modeling of an inverter-based DG for SC design purposes. In Section III the problem statement is given and the proposed SCs are outlined. Then, their performance features are analyzed by using Lyapunov tools. In Section IV the effectiveness of the proposed SCs is verified by simulating a realistic inverter-based MG with noisy measurements, parameter uncertainties and faults. Finally Section V provides concluding remarks and possible directions for further related investigations.

NOMENCLATURE

The adopted nomenclature of an inverter-based MG consisting of several interconnected DGs is defined hereinafter. The reader is referred to the Fig. 1 for a graphical explanation of the meaning of some variables.

ω_{com}	Speed of the common rotating ref. frame
ω_i	Local rotating ref. frame's speed of the *i*-th DG
δ_i	Angle between the local and the common rotating ref. frame, i.e., $\dot{\delta}_i = \omega_i - \omega_{com}$
$\omega_{ni}, \upsilon_{ni}$	Frequency and voltage droop-power setpoints
υ_{ki}, i_{ki}	3-ph voltages, currents at node *k* of the *i*-th DG
$\upsilon_{kdi}, \upsilon_{kqi}$	d-q voltages of the *i*-th DG at node *k*
i_{kdi}, i_{kqi}	d-q currents of the *i*-th DG at node *k*
$k = l, o, b$	input, output and branch local node of a DG
$\bar{\omega}, \bar{\upsilon}$	Rated values of MG's frequency and voltage
$\omega_{ref}, \upsilon_{ref}$	Desired values of frequency and voltage
P_i, Q_i	Active and reactive powers dc-components at the output node of the *i*-th DG
$\upsilon^*_{odi}, \upsilon^*_{oqi}$	d-q voltage setpoints of the *i*-th DG
ψ_{di}, ψ_{qi}	d-q voltage error's integral of the *i*-th DG
i^*_{ldi}, i^*_{lqi}	d-q current setpoints of the *i*-th DG
ϕ_{di}, ϕ_{qi}	d-q current error's integral of the *i*-th DG

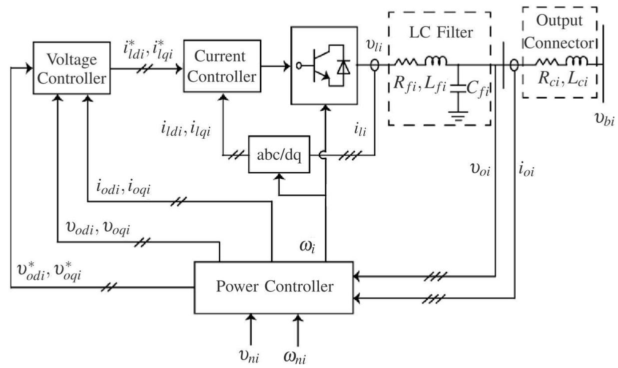

Fig. 1. Primary control block diagram of an inverter-based DG.

II. MG Modeling for Secondary Control Design

The block diagram of a DG with PC loops is shown in Fig. 1. It consists of a dc-ac power system consisting of a 3-ph inverter whose dc-side is connected to a dc source (e.g., photovoltaic panels [8], fuel cell system [23] or variable ac-dc wind turbines [9]), whereas the ac-side is connected to the 3-ph grid by the series of the coupling and the output filters.

The PC consists of three nested control loops that control, respectively, the power, voltage, and current injected in MG by each DG. The PC is generally formulated in the d-q (direct-quadrature) axes of the local reference frame rotating at ω_i [24]. Its aim is to stabilize the MG dynamics while preserving the load sharing among DGs. Role of the SC is to generate the references for the inner PCs, i.e., the signals ω_{ni} and υ_{ni}, such that ω_i and υ_{odi} are forced to converge to the respective setpoints ω_{ref} and υ_{ref}. In general the reference (ref.) frame of a specifically chosen DG is considered as the common ref. frame. Let ω_{com} be the rotating speed of the common ref. frame. The relative angle δ_i between the common ref. frame and the local ref. frame of the i-th DG is defined as follows

$$\frac{d\delta_i}{dt} = \omega_i - \omega_{\text{com}} \tag{1}$$

Based on droop techniques, the power control loops of the i-th DG [1] are governed by the relations

$$\omega_i = \omega_{ni} - m_i \cdot P_i \tag{2}$$
$$\upsilon^*_{odi} = \upsilon_{ni} - n_i \cdot Q_i \tag{3}$$
$$\upsilon^*_{oqi} = 0 \tag{4}$$

where m_i and n_i are the droop coefficients, whereas P_i and Q_i denote the dc-components of the instantaneous active and reactive local output power terms passed through a low-pass process with cut-off frequency $\omega_{ci} \ll \omega_i \leqslant \omega_{ni}$, i.e.,

$$\frac{dP_i}{dt} = -\omega_{ci}P_i + \omega_{ci}\left(\upsilon_{odi}\cdot i_{odi} + \upsilon_{oqi}\cdot i_{oqi}\right) \tag{5}$$
$$\frac{dQ_i}{dt} = -\omega_{ci}Q_i + \omega_{ci}\left(\upsilon_{oqi}\cdot i_{odi} - \upsilon_{odi}\cdot i_{oqi}\right) \tag{6}$$

[1] Without loss of generality, we consider the droop equations (2)-(3) without the TC's power set-points. If desired, these can be included by changing them as $\omega_i = \omega_{ni} - m_i(P_i - P_{i,ref})$ and $\upsilon^*_{odi} = \upsilon_{ni} - n_i(Q_i - Q_{i,ref})$.

Finally, the voltage and current PCs are PI-based and, particularly, the voltage control is governed by

$$\frac{d\psi_{di}}{dt} = k_{ivi}(\upsilon^*_{odi} - \upsilon_{odi}) \tag{7}$$
$$\frac{d\psi_{qi}}{dt} = k_{ivi}(\upsilon^*_{oqi} - \upsilon_{oqi}) \tag{8}$$
$$i^*_{ldi} = \psi_{di} + k_{pvi}(\upsilon^*_{odi} - \upsilon_{odi}) + k_{fvi}i_{odi} - \bar{\omega}C_{fi}\upsilon_{oqi} \tag{9}$$
$$i^*_{lqi} = \psi_{qi} + k_{pvi}(\upsilon^*_{oqi} - \upsilon_{oqi}) + k_{fvi}i_{oqi} + \bar{\omega}C_{fi}\upsilon_{odi} \tag{10}$$

whereas the current controller satisfies the next relations

$$\frac{d\phi_{di}}{dt} = k_{ici}(i^*_{ldi} - i_{ldi}) \tag{11}$$
$$\frac{d\phi_{qi}}{dt} = k_{ici}(i^*_{lqi} - i_{lqi}) \tag{12}$$
$$\upsilon^*_{ldi} = \phi_{di} + k_{pci}(i^*_{ldi} - i_{ldi}) - \bar{\omega}L_{fi}i_{lqi} \tag{13}$$
$$\upsilon^*_{lqi} = \phi_{qi} + k_{pci}(i^*_{lqi} - i_{lqi}) + \bar{\omega}L_{fi}i_{ldi} \tag{14}$$

where $\bar{\omega}$ is the rated frequency of the MG. L_{fi} and C_{fi} are the inductance and capacitance of the coupling filter and the triplets k_{pvi}, k_{ivi}, k_{fvi} and k_{pci}, k_{ici}, k_{fci} denote, resp., the proportional, integral and feedforward gains of these controllers.

Lastly, the dynamics of the LC filter and of the output connector of the i-th DG expressed in the local d-q axes are

$$\frac{di_{ldi}}{dt} = -\frac{R_{fi}}{L_{fi}}i_{ldi} + \frac{1}{L_{fi}}\left(\upsilon_{ldi} - \upsilon_{odi}\right) + \omega_i i_{lqi} \tag{15}$$
$$\frac{di_{lqi}}{dt} = -\frac{R_{fi}}{L_{fi}}i_{lqi} + \frac{1}{L_{fi}}\left(\upsilon_{lqi} - \upsilon_{oqi}\right) - \omega_i i_{ldi} \tag{16}$$
$$\frac{d\upsilon_{odi}}{dt} = \frac{1}{C_{fi}}\left(i_{ldi} - i_{odi}\right) + \omega_i \upsilon_{lqi} \tag{17}$$
$$\frac{d\upsilon_{oqi}}{dt} = \frac{1}{C_{fi}}\left(i_{lqi} - i_{oqi}\right) - \omega_i \upsilon_{ldi} \tag{18}$$
$$\frac{di_{odi}}{dt} = -\frac{R_{ci}}{L_{ci}}i_{odi} + \frac{1}{L_{ci}}\left(\upsilon_{odi} - \upsilon_{bdi}\right) + \omega_i i_{oqi} \tag{19}$$
$$\frac{di_{oqi}}{dt} = -\frac{R_{ci}}{L_{ci}}i_{oqi} + \frac{1}{L_{ci}}\left(\upsilon_{oqi} - \upsilon_{bqi}\right) - \omega_i i_{odi} \tag{20}$$

where υ_{bdi}, υ_{bqi} denote the voltages at the connection bus (see Fig. 1 and 2). Note that, υ^*_{ldi} and υ^*_{lqi} in (13) and (14) denote the smooth signals provided by inner current control, whereas υ_{ldi} and υ_{lqi} in (15) and (18) denote the effective non-smooth dispatched voltages of the inverter at the ac port after a high frequency PWM process. Due to the very high switching frequencies of power bridges, the inverter dynamics can safely be neglected, if compared to the MG dynamics. Thus, due to the averaging principle, and similarly to [15], [25], (13) and (14) can be safely substituted for υ_{ldi} and υ_{lqi} into the equations (15) and (16).

A compact 13-th order nonlinear model for the i-th DG operating over a MG system is thus obtained by combining equations (1)-(20), which yields the system

$$\dot{\boldsymbol{x}}_i = \boldsymbol{f}_i(\boldsymbol{x}_i) + \boldsymbol{g}_i(\boldsymbol{x}_i)\cdot\boldsymbol{u}_i + \boldsymbol{w}_i(\boldsymbol{x}_i)\boldsymbol{d}_i \tag{21}$$
$$\boldsymbol{x}_i = [\delta_i, P_i, Q_i, \phi_{di}, \phi_{qi}, \psi_{di}, \psi_{qi}, i_{ldi}, i_{lqi}, \upsilon_{odi}, \upsilon_{oqi}, i_{odi}, i_{oqi}]'$$

where $\boldsymbol{x}_i \in \mathbb{R}^{13}$ is the own state vector of the i-th DG, $\boldsymbol{u}_i = [\omega_{ni}, \upsilon_{ni}]' \in \mathbb{R}^2$ is its SC input and $\boldsymbol{d}_i = [\upsilon_{bdi}, \upsilon_{bqi}]' \in \mathbb{R}^2$ is considered as an unknown disturbances. Lastly, $\boldsymbol{f}_i(\boldsymbol{x}_i)$, $\boldsymbol{g}_i(\boldsymbol{x}_i)$, and $\boldsymbol{w}_i(\boldsymbol{x}_i)$ can easily be derived from (1) to (20).

Remark 1. *According to Fig. 2, the DGs dynamics are coupled each other due to the interconnecting power lines and are also affected by the local utilities. Although* (21) *does not show explicitly this coupling, these effects can be encoded by the bus voltages* υ_{bi} *[25], here assumed to be unknown. Differently from the present investigation, in [14], [15], [16], these quantities were assumed to be known and then compensated by feedback-linearization/feedforward techniques.* ■

In the following, we will distinguish between the interaction among DGs due to electrical power lines and the interaction due to the SC communication infrastructure [26], as in Fig. 2.

The *communication layer* is conveniently described by a connected undirected graph $\mathcal{G}(\mathcal{V},\mathcal{E},\mathcal{A})$ [21] where $\mathcal{V}=\{1,\dots,n\}$ is the labeling set of the "n" DGs, $\mathcal{E}\subseteq\{\mathcal{V}\times\mathcal{V}\}$ is the set of communication links, and $\mathcal{A}$ is the weighted adjacency matrix of $\mathcal{G}$, such that $a_{ij}=a_{ji}=1$ if nodes i and j can exchange their state information and $a_{ij}=0$ otherwise. The *set of communication neighbors of the i-th DG* is $\mathcal{N}_i=\{j\in\mathcal{V}:(i,j)\in\mathcal{E}\}$. Information on $\mathcal{G}$ is also encoded by the *Laplacian matrix* $\mathcal{L}=[\ell_{ij}]\in\mathbb{R}^{n\times n}$, whose entries are

$$\ell_{ij}=\begin{cases}|\mathcal{N}_i|, & \text{if } i=j,\\ -1, & \text{if } (i,j)\in\mathcal{E} \text{ and } i\neq j,\\ 0, & otherwise.\end{cases} \qquad (22)$$

Let $\mathbf{1}_n=[1,\dots,1]'\in\mathbb{R}^n$ and $\mathbf{0}_n=[0,\dots,0]'\in\mathbb{R}^n$, $\mathcal{L}$ is a symmetric, positive semi-definite matrix with a simple zero eigenvalue, and it is such that $\mathcal{L}\mathbf{1}_n=\mathbf{0}_n$.
From now on, the next assumption is assumed to be in force.

Assumption 1. *Consider a MG of "n" DGs operating under the primary control* (1)-(14). *In the reminder, we assume the instantaneous active and reactive powers at the output node "o" of each DG to be bounded by a-priori known constants* Π^P *and* Π^Q *according to*

$$\left|\upsilon_{odi}i_{odi}+\upsilon_{oqi}i_{oqi}\right|\leqslant\Pi^P \quad , \quad \left|\upsilon_{oqi}i_{odi}-\upsilon_{odi}i_{oqi}\right|\leqslant\Pi^Q \quad (23)$$

Remark 2. *The feasibility of Ass. 1 is justified by the fact that the instantaneous power flowing throughout the network is bounded everywhere, by the bounded operating range of the inverter voltages and currents.* ■

Due to Ass. 1 and to the uniform boundedness of the state of the first-order filters (5) and (6), P_i and Q_i will also be uniformly bounded. Thus, one can straightforwardly upper estimate the right-hand side of (5)-(6) as follows

$$\left|\dot{P}_i\right|\leqslant\dot{P}_\infty\equiv 2\omega_{ci}\Pi^P \quad , \quad \left|\dot{Q}_i\right|\leqslant\dot{Q}_\infty\equiv 2\omega_{ci}\Pi^Q \qquad (24)$$

For later use, an instrumental lemma is further presented.

Lemma 1. *Let us consider the Laplacian Matrix* $\mathcal{L}$ *associated to a connected undirected graph* $\mathcal{G}(\mathcal{V},\mathcal{E},\mathcal{A})$ *with "n" nodes. Let* $\boldsymbol{G}=\text{diag}([g_i])$ *be a diagonal matrix with all diagonal elements being nonnegative and at least one of them being strictly positive. Then,* $\boldsymbol{G}+\mathcal{L}$ *is a positive-definite matrix.* ■

Proof of Lemma 1. Let λ_i and $\zeta_i\in\mathbb{R}^n$, be the ordered eigenvalues of $\mathcal{L}$, i.e., $0=\lambda_1<\lambda_2\leqslant\cdots\leqslant\lambda_n$, and their associated eigenvectors. Any nonzero vector $\boldsymbol{z}=[z_i]\in\mathbb{R}^n$ can be expressed by $\boldsymbol{z}=\sum_{i=1}^n c_i\zeta_i$, for some arbitrary constants c_i. Since $\boldsymbol{G}$ has at least one non zero entry, $\exists\ i: g_i\neq 0$, it yields,

$$\boldsymbol{z}'\left(\boldsymbol{G}+\mathcal{L}\right)\boldsymbol{z}\geqslant\sum_{i=1}^n g_i z_i^2+\sum_{i=2}^n\lambda_i c_i^2\|\zeta_i\|_2^2\geqslant\sum_{i=1}^n g_i z_i^2\succ 0$$ ■

III. Distributed Control for Frequency and Voltage Secondary Restoration

A. Secondary Control Objectives

In the absence of a SC layer, it is well known (see e.g. [11]–[16]) that all the DG's frequencies and output voltages will deviates from their reference values. Following [11], [12], it is known that equation (2) enforces a steady-state ("ss") synchronization condition depending on the total active power flowing in the MG and on the droop coefficients, such that,

$$\lim_{t\to\infty}\omega_i(t)=\omega_{i,ss}=\omega_{ref}-\frac{\sum_{k=1}^n P_k}{\sum_{k=1}^n\frac{1}{m_k}} \quad \forall \quad i=1,\dots,n. \quad (25)$$

Due to (25), one derives that $\omega_{i,ss}=\omega_{j,ss}\Leftrightarrow m_iP_i=m_kP_k$ $\forall\ i,\ k\in\mathcal{V}$. Similarly, thanks to (3), the steady voltages will deviate from υ_{ref}. However, no voltage synchronization can be achieved [13]. It follows that, the purposes of the SC layer in an inverter-based MG of "n" DGs can be summarized as next:

1) Restore the frequencies and voltages of each DG to their reference values, i.e.,

$$\omega_{i,ss}=\omega_{ref} \quad \forall \quad i\in\mathcal{V} \qquad (26)$$
$$\upsilon_{odi,ss}=\upsilon_{ref} \quad \forall \quad i\in\mathcal{V} \qquad (27)$$

2) Guarantee the active power sharing ratio, i.e.,

$$P_{i,ss}/P_{k,ss}=m_k/m_i \quad \forall \quad i\in\mathcal{V} \qquad (28)$$

B. Distributed Secondary Controller Design

Strategies ranging from centralized to completely decentralized have been suggested to achieve the aforementioned SC purpose. However, centralized approaches conflict with the MG paradigm of autonomous management [13]. On the other hand, decentralized strategies appear to be unfeasible by using only local information [27]. As such, the communication between DGs has been identified as the key ingredient in achieving these goals while avoiding a centralized architecture. In accordance with the DT paradigm, and similarly to [12], [14], [15] and [16], we assume that at least one DG knows the voltage and frequency setpoints established by the TC. We also assume that the DGs may only communicate according to the communication graph $\mathcal{G}$.

1) Frequency Restoration Control: Thanks to the droop characteristic (2), and according to (25), the condition to achieve the frequency restoration (26), i.e., $\omega_{ref}=\omega_i=\omega_k$, while preserving the power sharing capabilities (28) is

$$\omega_{ni,ss}/\omega_{nk,ss}=1 \quad \forall \quad i,\ k=1,\dots,n \qquad (29)$$

In fact, except from special cases as e.g. [27], achieving the frequency synchronization without guaranteing (29) destroys the power sharing property established by the PC [12], [13], [27]. Achieving condition (26) subject to (29) is a more involved problem that cannot be solved by using standard consensus-based synchronization algorithms. Thus motivated, we propose the following novel sliding-mode based frequency restoration control strategy

$$\omega_{ni} = \tilde{\omega}_i + \bar{\omega} \tag{30}$$

$$\dot{\tilde{\omega}}_i = -\alpha \cdot \mathrm{sign}\left(\sum_{j \in \mathcal{N}_i} (\tilde{\omega}_i - \tilde{\omega}_j) + \sum_{j \in \mathcal{N}_i} (\omega_i - \omega_j) + g_i \left(\omega_i - \omega_{ref}\right) \right) \tag{31}$$

where $\bar{\omega}$ is the rated nominal MG's frequency, $\alpha \in \mathbb{R}^+$ is the protocol gain, $g_i \in \{0,1\}$ is the pinning gain, assumed to be equal to "1" for those DGs having direct access to the desired reference frequency ω_{ref} and "0" otherwise. Finally, the sign($\mathfrak{S}$) operator denotes the single-valued sign function

$$\mathrm{sign}(\mathfrak{S}) = \begin{cases} 1 & if \quad \mathfrak{S} > 0 \\ 0 & if \quad \mathfrak{S} = 0 \\ -1 & if \quad \mathfrak{S} < 0 \end{cases} \tag{32}$$

From (1)-(2), (30)-(31), a compact representation is straightforwardly derived as

$$\dot{\delta} = \omega - \omega_{com} = \tilde{\omega} + \mathbf{1}_n \otimes (\bar{\omega} - \omega_{com}) - \boldsymbol{m} \cdot \boldsymbol{P} \tag{33}$$

$$\dot{\tilde{\omega}} = -\alpha \cdot \mathrm{Sign}\left(\boldsymbol{\mathcal{L}} \left(\omega + \tilde{\omega}\right) + \boldsymbol{G}\left(\omega - \mathbf{1}_n \otimes \omega_{ref}\right)\right) \tag{34}$$

where $\otimes$ denotes the *Kronecker Product*, $\mathrm{Sign}(\mathfrak{S}) = [\mathrm{sign}(\mathfrak{S}_i)]$ is the column wise sign operator, $\tilde{\omega} = [\tilde{\omega}_i]$, $\omega = [\omega_i]$, $\boldsymbol{P} = [P_i]$ are vectors in $\mathbb{R}^n$, and $\boldsymbol{m} = \mathrm{diag}([m_i])$, $\boldsymbol{G} = \mathrm{diag}([g_i])$ are diagonal matrices in $\mathbb{R}^{n \times n}$ with entries $m_i > 0$ and $g_i \geqslant 0$. We are now in a position to state the first main result of this paper.

Theorem 1. *Consider a MG of "n" DGs, subject to the PC* (1)-(14)*, and communicating over a connected network* $\mathcal{G}$*. Let Ass. 1 be in force and let* $m_M = \max_i\{m_i\}$*, and let* μ_M *and* μ_m *be the maximum and minimum eigenvalues of matrix* $\boldsymbol{G} + \boldsymbol{\mathcal{L}}$*. If at least one DG has access to* ω_{ref}*, then the frequency controller* (30)-(31) *with*

$$\alpha > m_M \mu_M \dot{P}_\infty / \mu_m \tag{35}$$

ensures in finite-time the restoration condition (26)*, while preserving the power sharing accuracy condition* (28)*.* ■

Remark 3. *Some comments on the feasibility of the tuning rule* (35) *are given. In the right hand side of such relation, parameters* μ_M*,* μ_m *and* $\dot{P}_\infty$ *could be not obviously estimated. If* $\mathcal{G}$ *is fixed and known, then* μ_M *and* μ_m *are known as well. Otherwise, decentralized approaches are available to estimate them, see e.g. [28]. Concerning* $\dot{P}_\infty$*, relation* (24) *gives a conservative upper bound. However, one can observe that all signals in the right hand side of* (5) *are locally available for measurements, therefore distributed estimation strategies based on max-consensus [29] could be used to obtain less conservative estimations of this bound. Clearly, these strategies would be built on the same communication infrastructure of the SC layer.* ■

2) Voltage Restoration Control: With the aim of enhancing robustness to model uncertainties and convergence properties of the voltage restoration control loop, as compared to the previously quoted existing schemes, we propose a novel chattering-free SM distributed control protocol that guarantees the finite-time attainment of (27). Readers can refer to [30] for a comprehensive description of the Singular-Perturbation method, which is involved in the convergence proof.

As discussed in [12], [25], the cascaded voltage and current PCs in, resp., (7)-(10) and (11)-(14), are theoretically justified based on time-scale separation techniques. With this in mind, following the Singular Perturbation paradigm, let us make the realistic assumption that the inductance L_{fi} in (15), and the inverse of the integral gain of the current control $1/k_{ici}$ in (11) are small enough. Thus, we define $\varepsilon = \max\{L_{fi}, 1/k_{ici}\}$ as perturbation parameter. From (11), (13), (15), it yields

$$\varepsilon\left(\frac{d}{dt}\begin{bmatrix} i_{ldi} \\ \phi_{di} \end{bmatrix} - \begin{bmatrix} (\omega_i - \bar{\omega}) i_{lqi} \\ 0 \end{bmatrix}\right) = \begin{bmatrix} -R_{fi} - k_{pci} & 1 \\ -1 & 0 \end{bmatrix} \begin{bmatrix} i_{ldi} \\ \phi_{di} \end{bmatrix} + \begin{bmatrix} 1 \\ 1 \end{bmatrix} i^*_{ldi}$$

Setting $\varepsilon = 0$, as prescribed by the Singular Perturbation method, the quasi steady-state behavior of the fast dynamics are the solution of the resulting algebraic system, i.e.,

$$\begin{bmatrix} i_{ldi} \\ \phi_{di} \end{bmatrix} = \begin{bmatrix} 1 \\ -k_{pci} - R_{fi} - 1 \end{bmatrix} \cdot i^*_{ldi} \tag{36}$$

It follows that in the quasi-steady regime the current control forces the inverter to dispatch almost instantaneously its setpoint (9), in spite of the inherent coupling between the d-q components. Analogously, one also has that $i_{lqi} = i^*_{lqi}$.

Let us now consider the dynamics of the voltage variables to be restored. From (17) and (36) the reduced-order relation between υ_{odi} and the control input υ_{ni} is given by

$$\frac{d\upsilon_{odi}}{dt} = w_i(\omega_i, \psi_{di}, \upsilon_{odi}, \upsilon_{oqi}, i_{odi}) + \bar{w}_i \cdot \upsilon_{ni} \tag{37}$$

where $w_i = \left((\omega_i - \bar{\omega})\upsilon_{oqi} + \psi_{di} - k_{pvi}\upsilon_{odi} + (k_{fvi} - 1) i_{odi}\right)/C_{fi}$ and $\bar{w}_i = k_{pvi}/C_{fi}$. For later use, Lemma 2 is presented.

Lemma 2. *Consider a MG of "n" DGs, subject to the PC* (1)-(14)*. Let* (37) *be the dynamic equation of* υ_{odi} *in the quasi-steady regime of the current control. It follows that there exists* $\bar{\Omega}_i \in \mathbb{R}^+$ *such that* $|\dot{w}_i| \leqslant \bar{\Omega}_i$*,* $\forall\ i = 1, 2, ..., n$*.* ■

Proof of Lemma 2. Differentiating the expression of $w_i(\cdot)$ in (37), along the system dynamics (1)-(14) yields

$$\dot{w}_i = \dot{\omega}_i \upsilon_{oqi} + (\omega_i - \bar{\omega})\dot{\upsilon}_{oqi} - k_{pvi}\dot{\upsilon}_{odi} + (k_{fvi} - 1)\dot{i}_{odi} \tag{38}$$

From [11]–[16] follows that, thanks to the PC (1)-(14), the MG stability is guaranteed. Furthermore, the frequency synchronization on the value (25) is achieved. It follows that $\dot{\omega}_i$ is not only bounded but it decays to zero as well. That remains true a fortiori, also when the frequency SC (30)-(31) is active. Let us now consider the other terms in (38). With a similar line of reasoning as that of Ass. 1, due to the inherent boundedness of the MG variables in terms of generated and demanded power, and thanks to the stability established by the PC, υ_{odi}, υ_{oqi} and i_{odi} will also be bounded with bounded derivatives. Thus, we conclude that there exist a sufficiently large constant $\bar{\Omega}_i$, such that $|\dot{w}_i| \leqslant \bar{\Omega}_i$, $\forall\ i = 1, \ldots, n$. ■

We are now in a position to present the proposed novel sliding-mode based control for voltage restoration purposes

$$\dot{\upsilon}_{ni} = -\frac{C_{fi}}{k_{pvi}}\left[\varsigma_1 \cdot \text{sign}\left(\sum_{j\in\mathcal{N}_i}\left(\upsilon_{odi}-\upsilon_{odj}\right)+g_i\left(\upsilon_{odi}-\upsilon_{ref}\right)\right)\right.$$
$$\left.+\varsigma_2 \cdot \text{sign}\left(\sum_{j\in\mathcal{N}_i}\left(\dot{\upsilon}_{odi}-\dot{\upsilon}_{odj}\right)+g_i\left(\dot{\upsilon}_{odi}-\dot{\upsilon}_{ref}\right)\right)\right] \quad (39)$$

where $\varsigma_1,\ \varsigma_2 \in \mathbb{R}^+$ are the control gains, and $g_i \in \{0,1\}$ is the pinning gain, assumed to be equal to "1" if the i-th DG has a direct access to the reference voltage, "0" otherwise. Without loss of generality, we make the next assumption.

Assumption 2. *Let $\hat{\Omega} \in \mathbb{R}^+$ be a known positive constant. The reference voltage $\upsilon_{ref}(t)$ is such that $|\ddot{\upsilon}_{ref}(t)| \leqslant \hat{\Omega}$, $\forall\ t \geqslant 0$* ■

Theorem 2. *Consider a MG of "n" DGs, subject to the PC* (1)-(14)*, and communicating over a connected network $\mathcal{G}$. Let Ass. 1 and Ass. 2 be in force and let $\bar{\Omega}_M = \max_i |\dot{w}_i|$ with w_i as in* (38)*. If at least one DG has access to υ_{ref}, then the voltage controller* (39) *with*

$$\varsigma_1 > \varsigma_2 + \hat{\Omega} + \bar{\Omega}_M\ ,\ \ \varsigma_2 > \hat{\Omega} + \bar{\Omega}_M \quad (40)$$

ensures the finite voltage restoration (27). ■

Remark 4. *Some comments on the tuning rules* (40) *are given. Let us first note that υ_{ref} is a signal generated ad-hoc for SC purposes by higher level logics. Thus, its rate of variation can safely be assumed to be bounded and a-priori known by a constant $\hat{\Omega}$, as stated in Ass. 2. As for the estimation of $\bar{\Omega}_M = \max_i \bar{\Omega}_i$, first note that from Lemma 2 the local bounds $\bar{\Omega}_i$ exist. Furthermore, thanks to the PC stability properties [12], [25], and to the current and voltage operating limits, one can derive conservative estimations of $\bar{\Omega}_M$. However, better estimations of these quantities based on more sophisticated strategies can be devised. As an example, since* (38) *depends on measurable variables then the exact estimation of $\bar{\Omega}_i$ could be computed in a decentralized way by using, e.g., finite-time unknown input observers [31] or disturbance observers [32]. Alternatively, similarly to Remark 3, distributed estimation strategies based on max-consensus [29], could be used to cooperatively obtain less conservative estimations of this bound. Clearly these strategies would be built on the same communication infrastructure of the SC layer.* ■

Remark 5. *The chattering problem is a critical aspect in sliding mode control implementation. Several strategies have been proposed to counteract it, e.g., the introduction of observer-based auxiliary loops [33], the averaging of the discontinuities by low-pass filters [34], the use of higher order sliding mode algorithms [35], to cite a few. Here, an ad-hoc input dynamic extensions conceptually similar to that used in [36] is proposed. Thus, the secondary controllers* (30)-(31), *and* (39) *result in continuous control actions, thereby alleviating the chattering. However, due to unmodeled dynamics or to the finite sampling rate of digital controllers, small residual chattering may still appear [30]. Thus, following [37], a useful additional countermeasure is to smooth out the discontinuities by using smooth approximations of the sign functions such as, e.g., the sigmoidal approximation sign$(\mathfrak{S}) \approx \mathfrak{S}/(\mathfrak{S}+\varepsilon)$ with small parameter $\varepsilon \to 0$.* ■

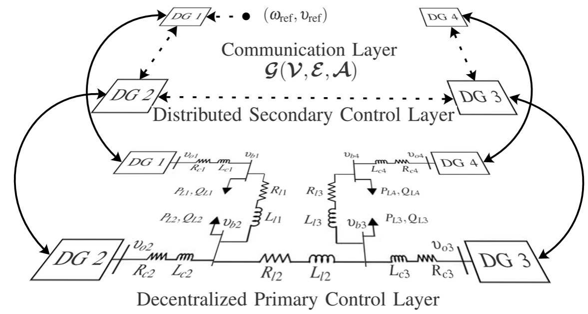

Fig. 2. Diagram of the considered MG control layers with four DGs.

TABLE I
SPECIFICATION OF THE MICROGRID TEST SYSTEM

DG's Parameters		DG 1	DG 2	DG 3	DG 4
Droop Control	m_p	10×10^{-5}	6×10^{-5}	4×10^{-5}	3×10^{-5}
	n_Q	1×10^{-2}	1×10^{-2}	1×10^{-2}	1×10^{-2}
Voltage Control	k_{pv}	0.4	0.4	0.4	0.4
	k_{iv}	500	500	500	500
	k_{fv}	0.5	0.5	0.5	0.5
Current Control	k_{pc}	0.4	0.4	0.4	0.4
	k_{ic}	700	700	700	700
LC Filter [Ω],[mH],[μF]	R_f	0.1	0.1	0.1	0.1
	L_f	1.35	1.35	1.35	1.35
	C_f	50	50	50	50
Connector [Ω],[mH]	R_c	0.03	0.03	0.03	0.03
	L_c	0.35	0.35	0.35	0.35
Lines [Ω],[μH]		Line 1	Line 2	Line 3	
		R_{l1} 0.23	R_{l2} 0.23	R_{l3} 0.23	
		L_{l1} 318	L_{l2} 324	L_{l3} 324	
Loads [kW],[kVar]		Load 1	Load 2	Load 3	Load 4
		P_{L1} 3	P_{L2} 3	P_{L3} 2	P_{L4} 3
		Q_{L1} 1.5	Q_{L2} 1.5	Q_{L3} 1.3	Q_{L4} 1.5

IV. VERIFICATION OF RESULTS

A. Test Rig Design

The proposed SC architecture is verified by means of a realistic Simscape™ Power Systems™ Specialized Technology-compliant MATLAB®/Simulink® modelization of a 3-ph MG [38]. Fig. 1 and Fig. 2 illustrate the diagram of the considered MG and the schematics of the inverter-based DG modelization.

The DG's modelization includes a 3-ph IGBT bridge with 10kVA of rated power provided by a 800V dc-source. PWM Generators with 2kHz carrier are used to control the switching devices. According to (2)-(14), (30)-(31), and (39), the PC and the SC are formulated in the local ref. frames [24]. On the contrary, the coupling filter (15)-(18), the output connector (19)-(20) and the power lines are modeled in the *abc* frame by using 3-ph Series RLC Branches and the loads as 3-ph Parallel RLC Loads. The current and voltage outputs of the PI controllers, as well as the PWM modules, are saturated in accordance with the DGs' rated powers, resp., 380V_{ph-ph}, 32A. All the MG's specifications are summarized in Table I.

Simulations were performed by using the Runge-Kutta fixed-step solver with sampling time $T_s = 2\mu$s, whereas the PC and SC algorithms have been discretized by using the larger sampling step of $\bar{T}_s = 0.5$ms. Finally, the secondary control gains are chosen as follows $\alpha = 200$, $\varsigma_1 = 240$, and $\varsigma_2 = 250$. Note that, in accordance with Remark 5, the sign function (32) is approximated by a sigmoidal function with $\varepsilon = 0.01$.

At the startup, the SC communication network $\mathcal{G}$ has the same topology of the power network, as in Fig. 2. DG 1 is the only DG that knows the reference voltage υ_{ref} and frequency ω_{ref}, i.e., $g_1 = 1$ and $g_2 = g_3 = g_4 = 0$ [12], [16].

To test the robustness of the algorithm, uncertainties in the range of $\pm(10 \div 15)\%$ of the corresponding nominal values are introduced for all the DG's parameters involved for control purposes, namely parameters C_{fi} and L_{fi} in (9)-(10) and (13)-(14). Realistic noisy measurements are also taken into account. Particularly, all measurements are converted into the $4 \div 20$mA range with power transmission equal to 0.2W, and then corrupted by an Additive White Gaussian Noise with a realistic Signal-to-Noise Ratio of 90dB [39].

Finally, in order to investigate the robustness of the proposed SC algorithms against sudden planned or unplanned events, the presence of load changes, 3-ph faults, and the consequent re-configuration of both the physical and the SC communication topologies are also scheduled throughout the simulation.

In particular, a 3-ph to ground fault [40] will be introduced on Line 3, i.e. R_{l3}, L_{l3}, see Fig. 2. Then, due to the surge transient current and according to the delays of protection devices, 10msec later, two circuit breakers located at the branch buses "$b3$" and "$b4$" will isolate DG 4 from the MG. Finally, two seconds later, the SC is also reconfigured by letting $a_{34} = a_{43} = 0$. Meanwhile, DG 4 continues to fed Load 4 with only its local PC active.

B. Case Study

The use-case under test schedules the next list of events:

I1 At the startup ($t = 0$s), only the PC is active with PC set-points $\omega_{ni} = 2\pi \cdot 50$Hz and $\upsilon_{ni} = 220\text{V}_{\text{RMS}} \approx 380\text{V}_{\text{ph-ph}}$;

I2 At $t = 5$s the frequency restoration SC (30)-(31) is activated with $\omega_{ref} = 2\pi \cdot 50$Hz;

I3 At $t = 10$s the voltage restoration SC (39) is activated with $\upsilon_{ref} = 220\text{V}_{\text{RMS}} \approx 380\text{V}_{\text{ph-ph}}$;

I4 By using a 3-ph breaker, Load 3, i.e. (P_{L3}, Q_{L3}), is connected at $t = 15$s, and removed at $t = 25$s;

I5 At $t = 30$s the SC frequency setpoint is changed to $\omega_{ref} = 2\pi \cdot 50.2$rad/s;

I6 At $t = 35$s the SC voltage setpoint is changed to $\upsilon_{ref} = 224\text{V}_{\text{RMS}} \approx 388\text{V}_{\text{ph-ph}}$;

I7 At $t = 40$s a 3-ph to ground fault occurs on the Line 3;

I8 At $t = 40.01$s over-current protection devices isolate the Line 3, and thus DG 4 and Load 4, from the MG;

I8 At $t = 42$s the SC is reconfigured to take into account the changes occurred at the physical layer, i.e., $a_{34} = a_{43} = 0$;

I9 At $t = 43$s the SC frequency setpoint is changed to $\omega_{ref} = 2\pi \cdot 50.2$rad/s;

I10 At $t = 44$s the SC voltage setpoint gets back to $\upsilon_{ref} = 220\text{V}_{\text{RMS}} \approx 380\text{V}_{\text{ph-ph}}$.

Let us now discuss the obtained results depicted from Fig. 3 to Fig. 8. In the first five seconds, the SC layer is switched off and only the PCs result to be active. From Fig. 3 and Fig. 4, during this period all the local voltages and frequencies deviate from the corresponding PC setpoints. The voltages also deviate each other. As expected, and in accordance with Fig. 4 and Fig. 5, the synchronization among frequencies to the common value (25), as well as the power sharing constraints (28) and (29) are achieved, as confirmed also by Fig. 6.

At $t = 5s$ the frequency SC (30)-(31) is activated. Fig. 4

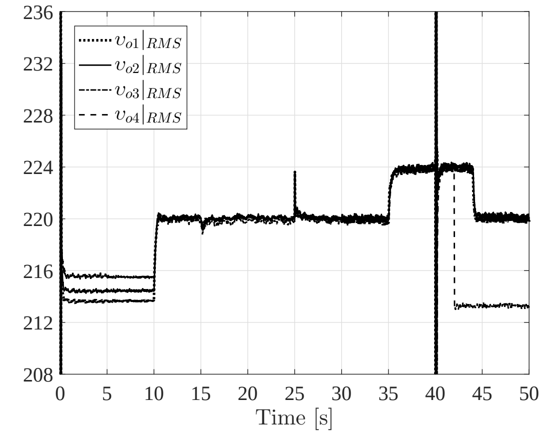

Fig. 3. RMS inverters' output voltages $\upsilon_{oi}(t)$.

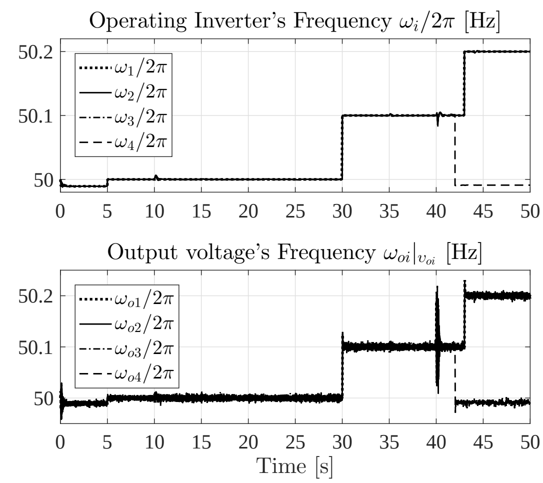

Fig. 4. Top: Inverters' operating frequencies ω_i. Bottom: Frequencies of the output voltage of each DG $\upsilon_{oi}(t)$ measured by a 3-phase PLL.

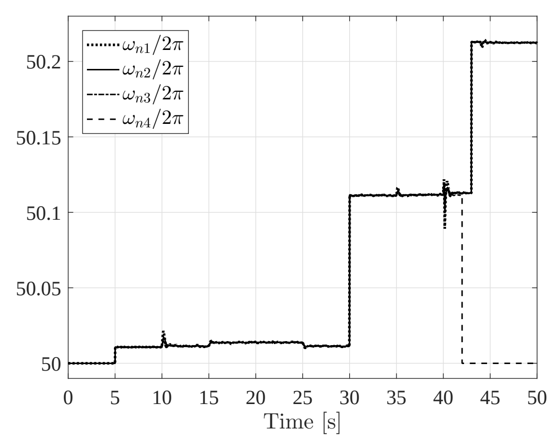

Fig. 5. Secondary frequency restoration control actions $\omega_{ni}(t)$.

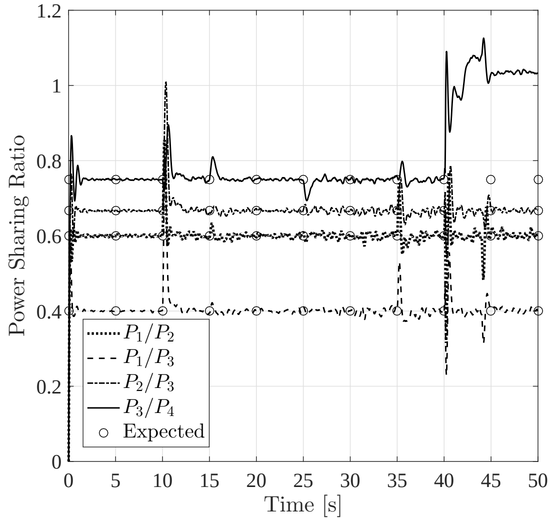

Fig. 6. Comparison between the expected, i.e. m_i/m_j, and actual, i.e.$P_i(t)/P_j(t)$, power sharing ratio, with $i = 1,2,3,4,\ j \neq i,\ j > i$.

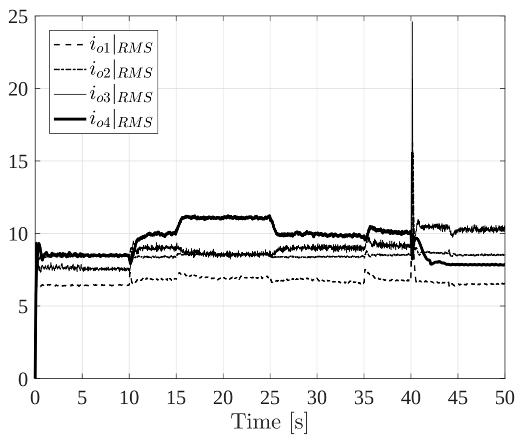

Fig. 7. RMS inverters' output currents $i_{oi}(t)$.

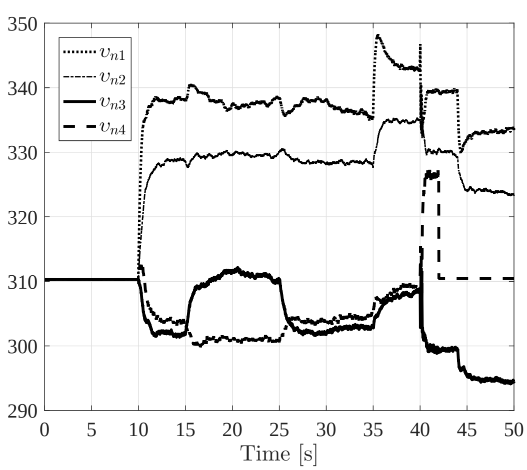

Fig. 8. Secondary voltage restoration control actions $\upsilon_{ni}(t)$.

shows that almost instantaneously the frequencies are restored in finite-time to the desired 50Hz value. From Fig. 5 it is also of interest to note that the agreement on the frequency SC actions, i.e. condition (29), is in force. It follows that the desired active power ratios are preserved, as shown in Fig. 6.

At $t = 10s$, the voltage restoration control (39) is activated. Fig. 3 shows that all the output voltages are quickly steered to the expected setpoint $\upsilon_{ref} = 220\text{V}_{\text{RMS}}$ in a distributed way.

At $t = 15$s and $t = 25$s, Load 3 is resp. connected and disconnected. Figures 3, 4 and 6 further show that, quickly after the load connection and disconnection instants, the voltage and frequency restoration, as well as the power sharing accuracy, are achieved in spite of abrupt changes in the power demand.

At $t = 30$s and $t = 35$s the SC setpoints are resp. changed to $\omega_{ref} = 2\pi \cdot 50.2$Hz and $\upsilon_{ref} = 224\text{V}_{\text{RMS}}$. Fig. 3 and Fig. 4 show that the new setpoints are achieved very quickly.

At $t = 40$s, Line 3 is grounded. Due to this fault, a surge current, depicted in Fig. 7 is generated. Then, 10ms later, protection devices isolate that portion of the MG. Although DG 4 and Load 4 have been electrically isolated from the rest of the MG, the SCs are intentionally reconfigured only two seconds later at $t = 42$s. From Figures 3, 4, 5, and 8, it can be noted that, even in spite of changes on the MG electrical topology (DG 4 has been isolated), the restoration control aims for all the DGs is still guaranteed, whereas, limited to those DGs that can share their loads, i.e. DG 1, DG 2 and DG 3, also the power sharing constraints are still in force.

At $t = 42$s the secondary communication layer is updated, i.e. $a_{34} = a_{43} = 0$, and DG 4 starts to operate with only the PC active, with $\omega_{n4} = 2\pi \cdot 50$Hz and $\upsilon_{n4} = 220\text{V}_{\text{RMS}}$, see Figs. 5 and 8. Finally, to show the tracking performances of the proposed SCs during the novel SC configuration, at $t = 43$s and $t = 44$s, the secondary setpoints are updated, resp., to $\omega_{ref} = 2\pi \cdot 50.2$Hz and $\upsilon_{ref} = 220\text{V}_{\text{RMS}}$. Finally, the time profiles of the SC actions $\omega_{ni}(t)$ and $\upsilon_{ni}(t)$, in Fig. 5 and Fig. 8 confirm that the chattering is successfully removed.

These simulation results confirm that the proposed SC schemes effectively accomplish all their goals by using local information from the neighboring DGs only. Simulations have further shown good voltage and frequency tracking performances in spite of parameter uncertainties, noisy measurements, and the occurrence of abrupt structural modification in both the electrical and the secondary communication layers.

V. Conclusions

Distributed tracking consensus algorithms to achieve voltage and frequency restoration in the SC layer of an islanded inverter-based MG have been proposed. Main improvement over the related literature can be stated in terms of performing the theoretical analysis by considering a faithful MG model during the controller design, while at the same time providing better convergence features and higher level of robustness against parameter uncertainties and exogenous perturbations.

Next activities will be targeted to relaxing the assumed restrictions on the communication topology by covering, e.g., directed and possibly switching or delayed communications [24]. Other interesting lines of investigation to be followed deal with the possibility to manage active loads, exploit seamless transfer strategies for MG from islanded to grid-connected mode [18] and investigating distributed asynchronous control techniques for managing power flows over large-scale MGs [41].

Experimental validations are also a natural continuation of the present research, that will allow a performance assessment of the proposed technique in a real scenario.

APPENDIX

Proof of Theorem 1. Define the argument of the $\mathrm{Sign}(\cdot)$ function in (34), as $\sigma_\omega = [\sigma_{\omega,i}] = \boldsymbol{\mathcal{L}}(\omega + \tilde{\omega}) + \boldsymbol{G}(\omega - \mathbf{1}_n \otimes \omega_{ref})$. It is straightforward to show that the constraint $\sigma_\omega = 0$ implies the achievement of both the control objectives (26) and (28). Thus, to prove Theorem 1, we must simply show the finite-time decaying to zero of σ_ω. Let us first differentiate σ_ω along the trajectory of the closed-loop dynamics (33)-(34)

$$\begin{aligned}\dot{\sigma}_\omega &= (\boldsymbol{G}+\boldsymbol{\mathcal{L}})\cdot\dot{\omega} + \boldsymbol{\mathcal{L}}\cdot\dot{\tilde{\omega}} \\ &= (\boldsymbol{G}+\boldsymbol{\mathcal{L}})\cdot\left(-\alpha\cdot\mathrm{Sign}(\sigma_\omega) + \boldsymbol{m}\cdot\dot{\boldsymbol{P}}\right) - \alpha\boldsymbol{\mathcal{L}}\cdot\mathrm{Sign}(\sigma_\omega)\end{aligned} \tag{41}$$

Let V_ω be a candidate Lyapunov function such that

$$V_\omega(t) = \|\sigma_\omega(t)\|_1 = \sum_{i=1}^{n} |\sigma_{\omega,i}(t)|\,. \tag{42}$$

By differentiating (42) along (41), and thanks to Lemma 1,

$$\begin{aligned}\dot{V}_\omega(t) &= \mathrm{Sign}(\sigma_\omega)'\dot{\sigma}_\omega \\ &\leqslant \mathrm{Sign}(\sigma_\omega)'((\boldsymbol{G}+\boldsymbol{\mathcal{L}})\cdot\left(-\alpha\cdot\mathrm{Sign}(\sigma_\omega) + \boldsymbol{m}\cdot\dot{\boldsymbol{P}}\right) \\ &\leqslant -\mathrm{Sign}(\sigma_\omega)'\left(\alpha\mu_m\cdot\mathrm{Sign}(\sigma_\omega) - \mu_M\boldsymbol{m}\cdot\dot{\boldsymbol{P}}\right)\end{aligned} \tag{43}$$

From (32), (42), it follows that $V_\omega \neq 0$ implies that there exist at least one $\sigma_{\omega,i} \neq 0$. Since $\alpha > m_M\mu_M\dot{P}_\infty/\mu_m$, follows that whenever $V_\omega(t) \neq 0$, (43) can be further estimated by

$$\begin{aligned}\dot{V}_\omega(t) &\leqslant -\sum_{i=1}^{n}\left(\alpha\mu_m\,\mathrm{sign}(\sigma_{\omega,i})^2 - m_M\mu_M\,\mathrm{sign}(\sigma_{\omega,i})\dot{P}_\infty\right) \\ &= -\sum_{\forall\ i\ :\ \sigma_{\omega,i}\neq 0}\left(\alpha\mu_m - m_M\mu_M\dot{P}_\infty\right) \leqslant -\rho \prec 0,\end{aligned} \tag{44}$$

where ρ is a strictly positive constant that define the minimum decaying rate of V_ω, when $V_\omega(t)$ is nonzero. On the contrary, if $\sigma_{\omega,i} = 0\ \forall\ i \in \boldsymbol{\mathcal{V}}$, then $V_\omega = 0$. Furthermore, from (44) σ_ω goes to zero in finite-time, while preserving (26) and (28). ■

Proof of Theorem 2. Let us define the error variables $\sigma_{\upsilon 1} = \boldsymbol{y}_1 - \mathbf{1}\otimes\upsilon_{ref}$, $\sigma_{\upsilon 2} = \boldsymbol{y}_2 - \mathbf{1}\otimes\dot{\upsilon}_{ref}$ where $\boldsymbol{y}_1 = [\upsilon_{odi}] \in \mathbb{R}^n$ and $\boldsymbol{y}_2 = [\dot{\upsilon}_{odi}] \in \mathbb{R}^n$. By differentiating $\sigma_{\upsilon 1}$ and $\sigma_{\upsilon 2}$ along the trajectories of (37)-(39), and due to the zero row sum property $\boldsymbol{\mathcal{L}}\mathbf{1} = \mathbf{0}$ of the Laplacian matrix, the collective error output voltage dynamic is

$$\begin{aligned}\dot{\sigma}_{\upsilon 1} &= \sigma_{\upsilon 2} \\ \dot{\sigma}_{\upsilon 2} &= \dot{\boldsymbol{w}} - \mathbf{1}\otimes\ddot{\upsilon}_{ref} - \varsigma_1\cdot\mathrm{Sign}((\boldsymbol{\mathcal{L}}+\boldsymbol{G})\sigma_{\upsilon 1}) \\ &\quad -\varsigma_2\cdot\mathrm{Sign}((\boldsymbol{\mathcal{L}}+\boldsymbol{G})\sigma_{\upsilon 2})\end{aligned} \tag{45}$$

where $\boldsymbol{w} = [w_i] \in \mathbb{R}^n$. By invoking Ass. 2 and Lemma 2, it follows that $\|\dot{\boldsymbol{w}} - \mathbf{1}\otimes\ddot{\upsilon}_{ref}\|_\infty \leqslant \hat{\Omega} + \max_{i\in\boldsymbol{\mathcal{V}}}\bar{\Omega}_i \equiv \Omega$. Let $\boldsymbol{\mathcal{M}} = \boldsymbol{G} + \boldsymbol{\mathcal{L}} \in \mathbb{R}^{n\times n}$ and because by assumption at least one DG has a direct access to the reference voltage, from Lemma 1, $\boldsymbol{\mathcal{M}} \succ 0$. Thus, let us consider as candidate Lyapunov function $V_\upsilon(t) = \varsigma_1\cdot\|\boldsymbol{\mathcal{M}}\sigma_{\upsilon 1}\|_{\mathbf{1}} + \frac{1}{2}\cdot\sigma_{\upsilon 2}'\boldsymbol{\mathcal{M}}\sigma_{\upsilon 2} \succ 0$. By performing computations similar to those made in [42] for a leaderless network of double integrators, i.e. such that $\boldsymbol{G} = 0$, it results

$$\dot{V}_\upsilon(t) \leqslant -(\varsigma_{\upsilon 2} - \Omega)\cdot\|\boldsymbol{\mathcal{M}}\sigma_{\upsilon 2}\|_{\mathbf{1}} \preceq 0 \quad \text{if} \quad \varsigma_{\upsilon 2} > \Omega. \tag{46}$$

By virtue of (46), the equi-uniform stability of the error dynamic (45) is thus established. Let $R > V_\upsilon(0)$, by (46), it further follows that, whenever system (45) will be initialized in an arbitrary vicinity of the origin, the corresponding solution is confined within the invariant set $\boldsymbol{\mathcal{D}}_R = \{(\sigma_{\upsilon 1}, \sigma_{\upsilon 2}) \in \mathbb{R}^{2n}\ :\ V_\upsilon(\sigma_{\upsilon 1}, \sigma_{\upsilon 2}) \leqslant R\}$. Let μ_m be the smallest eigenvalue of $\boldsymbol{\mathcal{M}}$, and $\kappa_R > 0$ be sufficiently small such that $\kappa_R < \min\{2\varsigma_1^2/R, \mu_m, \sqrt{\mu_m/2R}\cdot(\varsigma_2 - \Pi)\}$. By invoking the Extended Invariance Principle, as in [42], the augmented Lyapunov function $W_\upsilon(t) = V_\upsilon(t) + \kappa_R\cdot\sigma_{\upsilon 1}'\boldsymbol{\mathcal{M}}\sigma_{\upsilon 2}$ satisfies

$$W_\upsilon(t) \geqslant \underline{c}_R\cdot(\|\boldsymbol{\mathcal{M}}\sigma_{\upsilon 1}\|_{\mathbf{1}} + \|\boldsymbol{\mathcal{M}}\sigma_{\upsilon 2}\|_{\mathbf{1}}) \succ 0 \tag{47}$$

with $\underline{c}_R = \min\{\varsigma_1 - \kappa_R R/(2\varsigma_1), (\mu_m - \kappa_R)/2\}$. Lengthy but straightforward computations yield that $W_\upsilon(t) \leqslant \bar{c}_R\cdot(\|\boldsymbol{\mathcal{M}}\sigma_{\upsilon 1}\|_{\mathbf{1}} + \|\boldsymbol{\mathcal{M}}\sigma_{\upsilon 2}\|_{\mathbf{1}})$ with $\bar{c}_R = \max\{\varsigma_1 + \kappa_R\sqrt{2R/\mu_m}, \sqrt{R/(2\mu_m)}\}$. Finally, after differentiation of (47) along the system trajectories described by (45), the following estimation is shown to be in force

$$\frac{d}{dt}W_\upsilon(t) \leqslant -\left(\frac{c_R}{\bar{c}_R}\right)\cdot W_\upsilon(t) \tag{48}$$

with $c_R = \min\{\kappa_R(\varsigma_1 - \varsigma_2 - \Omega), \varsigma_2 - \Omega - \kappa_R\sqrt{2R/\mu_m}\} > 0$.

From (48), the augmented Lyapunopv function W_υ exponentially decays to zero. Due to the exponential stability of (45), and thanks to the uniform boundedness of the term $\|\dot{\boldsymbol{w}} - \mathbf{1}\otimes\ddot{\upsilon}_0\|_\infty \leqslant \Omega$ in (45), by invoking the Quasi-Homogeneity Principle [42, Theorem 2], it follows that $W_\upsilon(t)$ decays to zero in finite-time. Thus the errors variables $\sigma_{\upsilon 1}$ and $\sigma_{\upsilon 2}$ go to zero as well, while guaranteeing the voltage restoration (27). This conclude the proof. ■

REFERENCES

[1] D. E. Olivares, A. Mehrizi-Sani, A. H. Etemadi, C. A. Canizares, R. Iravani, M. Kazerani, A. H. Hajimiragha, O. Gomis-Bellmunt, M. Saeedifard, R. Palma-Behnke *et al.*, "Trends in microgrid control," *IEEE Trans. Smart Grid, 5(4), 1905–1919*, 2014.

[2] J. P. Lopes, C. Moreira, and A. Madureira, "Defining control strategies for microgrids islanded operation," *IEEE Trans. Power Syst., 21(2), 916–924*, 2006.

[3] J. W. Simpson-Porco, F. Dörfler, and F. Bullo, "Voltage stabilization in microgrids via quadratic droop control," *IEEE Trans. Autom. Control, 62(3), 1239–1253*, 2017.

[4] A. Bidram and A. Davoudi, "Hierarchical structure of microgrids control system," *IEEE Trans. Power Syst., 3(4), 1963–1976*, 2012.

[5] J. M. Guerrero, M. Chandorkar, T.-L. Lee, and P. C. Loh, "Advanced control architectures for intelligent microgrids: Decentralized and hierarchical control," *IEEE Trans. Ind. Electron., 60(4), 1254–1262*, 2013.

[6] F. Dörfler, J. W. Simpson-Porco, and F. Bullo, "Breaking the hierarchy: Distributed control and economic optimality in microgrids," *IEEE Trans. Control Netw. Syst., 3(3), 241–253*, 2016.

[7] J. Qin, Q. Ma, Y. Shi, and L. Wang, "Recent advances in consensus of multi-agent systems: A brief survey," *IEEE Trans. Ind. Electron., 64(6), 4972-4983.*, 2016.

[8] H. Xin, Z. Qu, J. Seuss, and A. Maknouninejad, "A self-organizing strategy for power flow control of photovoltaic generators in a distribution network," *IEEE Trans. on Power Syst., 26(3), 1462–1473*, 2011.

[9] F. Guo, C. Wen, J. Mao, and Y.-D. Song, "Distributed economic dispatch for smart grids with random wind power," *IEEE Trans. Smart Grid, 7(3), 1572–1583*, 2016.

[10] Q. Shafiee, J. M. Guerrero, and J. C. Vasquez, "Distributed secondary control for islanded microgrids - a novel approach," *IEEE Trans. Power Electron., 29(1), 1018–1031*, 2014.

[11] J. W. Simpson-Porco, F. Dörfler, and F. Bullo, "Synchronization and power sharing for droop-controlled inverters in islanded microgrids," *Elsevier, Automatica, 49(9), 2603–2611*, 2013.

[12] F. Guo, C. Wen, J. Mao, and Y.-D. Song, "Distributed secondary voltage and frequency restoration control of droop-controlled inverter-based microgrids," *IEEE Trans. Ind. Electron., 62(7), 4355–4364*, 2015.

[13] J. W. Simpson-Porco, Q. Shafiee, F. Dörfler, J. C. Vasquez, J. M. Guerrero, and F. Bullo, "Secondary frequency and voltage control of islanded microgrids via distributed averaging," *IEEE Trans. Ind. Electron., 62(11), 7025–7038*, 2015.

[14] A. Bidram, A. Davoudi, F. L. Lewis, and Z. Qu, "Secondary control of microgrids based on distributed cooperative control of multi-agent systems," *IET Gen., Transm. & Distrib., 7(8), 822–831*, 2013.

[15] A. Bidram, A. Davoudi, F. L. Lewis, and J. M. Guerrero, "Distributed cooperative secondary control of microgrids using feedback linearization," *IEEE Trans. Power Syst., 28(3), 3462–3470*, 2013.

[16] A. Bidram, A. Davoudi, F. L. Lewis, and S. S. Ge, "Distributed adaptive voltage control of inverter-based microgrids," *IEEE Trans. Energy Convers., 29(4), 862–872*, 2014.

[17] A. Jadbabaie, J. Lin, and A. S. Morse, "Coordination of groups of mobile autonomous agents using nearest neighbor rules," *IEEE Trans. Autom. Control, 48(6), 988-1001*, 2003.

[18] F. Tang, J. M. Guerrero, J. C. Vasquez, D. Wu, and L. Meng, "Distributed active synchronization strategy for microgrid seamless reconnection to the grid under unbalance and harmonic distortion," *IEEE Trans. Smart Grid, 6(6), 2757–2769*, 2015.

[19] Q.-C. Zhong, "Robust droop controller for accurate proportional load sharing among inverters operated in parallel," *IEEE Trans. Ind. Electron., 60(4), 1281–1290*, 2013.

[20] J. Schiffer, T. Seel, J. Raisch, and T. Sezi, "Voltage stability and reactive power sharing in inverter-based microgrids with consensus-based distributed voltage control," *IEEE Trans. Control Syst. Technol., 24(1), 96–109*, 2016.

[21] A. Pilloni, M. Franceschelli, A. Pisano, and U. Usai, "Recent advances in sliding-mode based consensus strategies," in *IEEE Int. W. Variable Structure Syst., 1(1), 1–6*, 2014.

[22] J. Mei, W. Ren, and G. Ma, "Distributed coordinated tracking with a dynamic leader for multiple euler-lagrange systems," *IEEE Trans. Autom. Control, 56(6), 1415–1421*, 2011.

[23] J. Liu, S. Vazquez, L. Wu, A. Marquez, H. Gao, and L. G. Franquelo, "Extended state observer-based sliding-mode control for three-phase power converters," *IEEE Trans. Ind. Electron. 64(1), 22–31*, 2017.

[24] C. Ahumada, R. Cárdenas, D. Saez, and J. M. Guerrero, "Secondary control strategies for frequency restoration in islanded microgrids with consideration of communication delays," *IEEE Trans. Smart Grid, 7(3), 1430–1441*, 2016.

[25] N. Pogaku, M. Prodanovic, and T. C. Green, "Modeling, analysis and testing of autonomous operation of an inverter-based microgrid," *IEEE Trans. Power Electron., 22(2), 613–625*, 2007.

[26] Y. Yan, Y. Qian, H. Sharif, and D. Tipper, "A survey on smart grid communication infrastructures: Motivations, requirements and challenges," *IEEE Commun. Surveys Tuts., 15(1), 5–20*, 2013.

[27] M. Andreasson, D. V. Dimarogonas, H. Sandberg, and K. H. Johansson, "Distributed control of networked dynamical systems: Static feedback, integral action and consensus," *IEEE Trans. Autom. Control, 59(7), 1750–1764*, 2014.

[28] M. Franceschelli, A. Gasparri, A. Giua, and C. Seatzu, "Decentralized estimation of laplacian eigenvalues in multi-agent systems," *Elsevier. Automatica, 49(4), 1031–1036*, 2013.

[29] J. Cortés, "Finite-time convergent gradient flows with applications to network consensus," *Elsevier. Automatica, 42(11), 1993–2000*, 2006.

[30] H. K. Khalil, "Nonlinear systems," *Prentice Hall, Pearson Educ.*, 2002.

[31] A. Pilloni, A. Pisano, E. Usai, P. P. Menon, and C. Edwards, "Decentralized state estimation in connected systems," *Elsevier. IFAC Proc. Volumes, 46(2), 421–426*, 2013.

[32] J. Yang, S. Li, and X. Yu, "Sliding-mode control for systems with mismatched uncertainties via a disturbance observer," *IEEE Trans. Ind. Electron., 60(1), 160–169*, 2013.

[33] V. Utkin and H. Lee, "Chattering problem in sliding mode control systems," in *IEEE Int. W. Variable Structure Syst., 1(1), 346–350*, 2006.

[34] V. Utkin and J. Shi, "Integral sliding mode in systems operating under uncertainty conditions," in *IEEE Conf. Decision and Control, 4(1), 4591–4596*, 1996.

[35] A. Levant, "Sliding order and sliding accuracy in sliding mode control," *Taylor & Francis. Int. J. Control, 58(6), 1247–1263*, 1993.

[36] A. Pilloni, A. Pisano, Y. Orlov, and E. Usai, "Consensus-based control for a network of diffusion pdes with boundary local interaction," *IEEE Trans. Autom. Control, 61(9), 2708–2713*, 2016.

[37] C. Edwards and S. Spurgeon, *Sliding mode control: theory and applications*. Crc Press, 1998.

[38] MathWorks, "Simscape power systems: Model and simulate electrical power systems," *http://it.mathworks.com/products/simpower/*, 2016.

[39] M. Pachchigar, "Complete sensor-to-bits solution simplifies industrial data-acquisition system design," *Analog Dialogue-Tech. Mag. Analog Devices, 47(2), 21–24*, 2013.

[40] Mathworks, "Three-phase fault:implement programmable phase-to-phase and phase-to-ground fault breaker system," *Documentation MATLAB® R2017a*, 2017. [Online]. Available: it.mathworks.com/help/physmod/sps/powersys/ref/threephasefault.html

[41] D. I. Koukoula and N. D. Hatziargyriou, "Gossip algorithms for decentralized congestion management of distribution grids," *IEEE Trans. Sustain. Energy, 7(3), 1071–1080*, 2016.

[42] A. Pilloni, A. Pisano, M. Franceschelli, and E. Usai, "Finite-time consensus for a network of perturbed double integrators by second-order sliding mode technique," *IEEE Conf. Decision and Control, 1(1), 2145-2150*, 2013.

Alessandro Pilloni was born in 1984. He received the Laurea degree (M.Sc) with honors in Electronic Eng. and the Ph.D. degree in Industrial Eng. from the University of Cagliari (Italy), in 2010 and 2014. He currently holds a research fellow position at the Dept. of Electrical and Electronic Eng., University of Cagliari. His research areas include variable structure control and their applications to nonlinear uncertain or distributed parameter systems, renewable distributed generation, fault-detection, consensus-based coordination of multi-agent networks. He has spent visiting periods at Universities and Research Centers in Spain, United Kingdom and Serbia. He is reviewer for several international conferences and journals, such as e.g., IEEE Trans. Autom. Control, Trans. Power Electron., Trans. Control Syst. Technol., Automatica (Elsevier).

Alessandro Pisano (M'07) was born in 1972. He graduated in Electronic Eng. in 1997 at the Dept. of Electrical and Electronic Eng. of the Cagliari University (Italy), where he received the Ph.D. degree in Electronics and Computer Science in 2000. He currently holds a position as assistant professor at DIEE. His current research interests include nonlinear control theory and its applications to nonlinear, uncertain and/or distributed parameter systems. He has authored/co-authored one book, 57 journal publications, 10 book chapters, and 105 papers in peer-reviewed international conference proceedings, and he is the holder of 4 patents. He has spent visiting periods at Universities and Research Centers in Belgium, France, Serbia and Mexico. He is Associate Editor of the Asian J. of Control and IEEE Control System Society Conference Editorial Board.

Elio Usai (M'96) is currently associate professor at the Dept. of Electrical and Electronic Eng. (DIEE), University of Cagliari, where he received the Laurea degree (M.Sc) in Electrical Eng. in 1985. He worked as process engineer first and then as production manager for international companies until 1994, when he joined DIEE as an assistant professor. Current interests are in output-feedback control, state estimation and FDI via higher order sliding modes in linear, nonlinear and infinite dimensional systems with uncertainties. He is co-author of more than 150 articles in international journals and conferences. He was General Chairperson of VSS'06, and he currently is Associate Editor for Asian Journal of Control, IEEE Transaction on Control System Technology and Journal of the Franklin Institute.